

SIRT3 Opposes Reprogramming of Cancer Cell Metabolism through HIF1 α Destabilization

Lydia W.S. Finley,¹ Arkaitz Carracedo,^{2,3} Jaewon Lee,¹ Amanda Souza,⁴ Ainara Egia,² Jiangwen Zhang,⁵ Julie Teruya-Feldstein,⁶ Paula I. Moreira,⁷ Sandra M. Cardoso,⁷ Clary B. Clish,⁴ Pier Paolo Pandolfi,² and Marcia C. Haigis^{1,*}

¹Department of Pathology, The Paul F. Glenn Labs for the Biological Mechanisms of Aging, Harvard Medical School, Boston, MA 02115, USA

²Cancer Genetics Program, Beth Israel Deaconess Cancer Center, Departments of Medicine and Pathology, Beth Israel Deaconess Medical Center, Harvard Medical School, Boston, MA 02215, USA

³CIC bioGUNE, Technology Park of Bizkaia, Derio 48160, Spain

⁴Metabolite Profiling Initiative, The Broad Institute of MIT and Harvard, Cambridge, MA 02142, USA

⁵Faculty of Arts and Sciences, Center for Systems Biology, Harvard University, Cambridge, MA 02138, USA

⁶Department of Pathology, Sloan-Kettering Institute, Memorial Sloan-Kettering Cancer Center, New York, NY 10065, USA

⁷Center for Neuroscience and Cell Biology, University of Coimbra, Coimbra 3004-517, Portugal

*Correspondence: marcia_haigis@hms.harvard.edu

DOI 10.1016/j.ccr.2011.02.014

SUMMARY

Tumor cells exhibit aberrant metabolism characterized by high glycolysis even in the presence of oxygen. This metabolic reprogramming, known as the Warburg effect, provides tumor cells with the substrates required for biomass generation. Here, we show that the mitochondrial NAD-dependent deacetylase SIRT3 is a crucial regulator of the Warburg effect. Mechanistically, SIRT3 mediates metabolic reprogramming by destabilizing hypoxia-inducible factor-1 α (HIF1 α), a transcription factor that controls glycolytic gene expression. SIRT3 loss increases reactive oxygen species production, leading to HIF1 α stabilization. SIRT3 expression is reduced in human breast cancers, and its loss correlates with the upregulation of HIF1 α target genes. Finally, we find that SIRT3 overexpression represses glycolysis and proliferation in breast cancer cells, providing a metabolic mechanism for tumor suppression.

INTRODUCTION

Otto Warburg first noted in the 1920s that cancer cells undergo glycolysis even in the presence of ample oxygen (Warburg, 1956). This preferential use of aerobic glycolysis, termed the Warburg effect, has emerged as a metabolic hallmark of many cancers. As a result, there is much interest in understanding the pathways that regulate the potential survival and proliferative advantages conferred by increased glucose uptake and catabolism, and this topic has been extensively reviewed (Tennant et al., 2010; Vander Heiden et al., 2009). Accruing evidence suggests that aerobic glycolysis is used to support the rapid

proliferation of tumor cells. Enhanced catabolism of glucose contributes to the raw materials needed to synthesize the nucleotides, amino acids, and lipids necessary for cellular proliferation and can provide a distinct growth advantage for cells with elevated aerobic glycolysis (Tong et al., 2009). Constitutive upregulation of aerobic glycolysis can also provide a survival advantage for tumor cells because limitations in tumor vascularization result in periods of intermittent hypoxia that require a cell to rely on glycolysis (Gatenby and Gillies, 2004). In support of this notion, the transition from premalignant lesions to invasive cancer is often accompanied by increased tumor glucose uptake (Gatenby and Gillies, 2004).

Significance

The dysregulation of cell metabolism is a unique and defining feature of many tumor cells. Thus, identifying factors that regulate cancer cell metabolism will enhance our understanding of how tumors hijack metabolism for selective advantages and provide approaches for cancer therapy. We find that loss of SIRT3, a sirtuin with NAD-dependent deacetylase activity, stabilizes HIF1 α and shifts cellular metabolism toward increased glycolysis, a common metabolic switch in cancer cells. Importantly, we also show that SIRT3 overexpression represses the Warburg effect. Our studies identify a high rate of SIRT3 deletion in human cancers and suggest that SIRT3 may be an important therapeutic target.

Metabolic reprogramming in cancer cells is regulated by several oncogenic cues, including the PI3K/Akt, Myc, or hypoxia-inducible factor (HIF) pathways that serve to increase glucose uptake, glycolysis, angiogenesis, and stress resistance (Kaelin and Ratcliffe, 2008; Semenza, 2010; Tennant et al., 2010; Tong et al., 2009). Recently, mutations in mitochondrial enzymes have emerged as important drivers of altered tumor cell metabolism. For example, gain- or loss-of-function mutations in tricarboxylic acid (TCA) cycle enzymes regulate HIF1 activity and promote carcinogenesis (Gottlieb and Tomlinson, 2005; Zhao et al., 2009). In turn, identification of new mitochondrial regulators of global cellular reprogramming could provide important insight into the contribution of altered metabolism to tumorigenesis.

Sirtuins are a conserved family of NAD-dependent ADP-ribosyltransferases and/or protein deacetylases involved in metabolism, stress response, and longevity (Finkel et al., 2009). Mammals express seven sirtuins (SIRT1–7), three of which (SIRT3–5) are localized to the mitochondrion. SIRT3 is a major mitochondrial deacetylase that targets many enzymes involved in central metabolism, resulting in the activation of many oxidative pathways (Verdin et al., 2010). For example, SIRT3 deacetylates complex I and complex II to activate electron transport (Ahn et al., 2008; Cimen et al., 2010). SIRT3 induces fatty acid oxidation during fasting in hepatocytes via deacetylation of LCAD (Hirschey et al., 2010). SIRT3 also targets the mitochondrial enzymes IDH2 and MnSOD (Qiu et al., 2010; Schlicker et al., 2008; Someya et al., 2010; Tao et al., 2010), which function in part to maintain reactive oxygen species (ROS) homeostasis. SIRT3 loss increases ROS levels and contributes to numerous age-related pathologies, including hearing loss and tumorigenesis (Kim et al., 2010; Someya et al., 2010). Previously, it was shown that SIRT3 functions as a tumor suppressor by decreasing ROS and maintaining genomic stability (Kim et al., 2010). In this study it was also demonstrated that SIRT3 null cells display increased glucose uptake and altered mitochondrial oxidation, but the direct contribution of SIRT3-mediated metabolic regulation on tumor growth remains a central question. Due to the pivotal role of SIRT3 as a regulator of ROS and multiple mitochondrial pathways, we sought to specifically probe the role of SIRT3 in regulating tumor cell metabolism and growth.

RESULTS

SIRT3 Promotes Cellular Metabolic Reprogramming

Because SIRT3 activates enzymes involved in mitochondrial fuel catabolism (Verdin et al., 2010), and SIRT3 loss increases glucose uptake (Kim et al., 2010), we hypothesized that SIRT3 could serve as an important regulator of the balance between glycolytic and anabolic pathways and mitochondrial oxidative metabolism to regulate tumor cell growth. To test this idea we first examined the influence of SIRT3 loss on metabolites from mouse embryonic fibroblasts (MEFs) using liquid chromatography-mass spectrometry (LC-MS). The metabolic profile of SIRT3 null (KO) MEFs demonstrated a clear shift toward glycolytic metabolism when compared with SIRT3 wild-type (WT) counterparts (Figure 1A), similar to the metabolic shift reported for transformed cells in culture (Lu et al., 2010) and for cancer

cells in vivo (Denkert et al., 2008; Hirayama et al., 2009). In SIRT3 KO cells, intermediates of glycolysis were elevated, whereas TCA cycle metabolites were reduced (Figures 1B and 1C). Consistent with a pattern of increased glucose usage, SIRT3 KO cells had lower levels of intracellular glucose (Figure 1D), whereas levels of glucose-1-phosphate, a product of glycogenolysis, were increased (Figure 1E). Glucose-1-phosphate can be converted by phosphoglucomutase into glucose-6-phosphate (G6P) to provide substrates for glycolysis or the oxidative arm of the pentose phosphate pathway (PPP), generating NADPH and ribose. The nonoxidative arm of the PPP forms ribose-5-phosphate from fructose-6-phosphate or glyceraldehyde-3-phosphate (Figure 1A). Importantly, G6P, glycolytic intermediates, and ribose-5-phosphate were all increased in SIRT3 KO cells (Figures 1A and 1F), suggesting that glucose metabolites were diverted into the PPP in order to provide the ribose necessary for nucleic acid synthesis. Notably, the pattern and the magnitude of metabolomic changes caused by SIRT3 loss were similar to those observed comparing tumors to nearby normal tissue (Hirayama et al., 2009).

Increased metabolites involved in glycolysis and the PPP suggested that, like many cancer cells, SIRT3 KO MEFs might be using glucose to support increased proliferation by directing glucose away from the TCA cycle toward biosynthetic processes. Indeed, SIRT3 KO cells grew significantly faster than WT cells (Figure 1G). To test whether this increased growth rate required aerobic metabolism of glucose, we grew cells in media containing galactose instead of glucose, thereby reducing glycolytic flux and forcing the cell to rely on mitochondrial oxidative phosphorylation (Marroquin et al., 2007). Under these conditions, WT and KO cells grew at the same rate, demonstrating that the increased proliferation of KO cells required enhanced glucose catabolism (Figure 1H).

To confirm that the metabolite patterns reflected an increase in glycolysis, we measured glucose uptake and lactate production. As expected, SIRT3 KO MEFs consumed more glucose and extruded more lactate into the media than did WT cells (Figures 1I and 1J). This effect was not specific to MEFs; HEK293T cells in which SIRT3 expression was stably reduced by lentiviral expression of shRNA against SIRT3 also showed an increase in glucose uptake and lactate production (see Figures S1A and S1B available online). Interestingly, the effect of SIRT3 loss on glucose uptake and lactate production was similar to the effect of pyruvate kinase M2 isoform overexpression or mTOR activation (Christofk et al., 2008; Duvel et al., 2010). These data suggest that loss of SIRT3 redirects cellular metabolism in favor of glycolysis, and as a result, cells with low levels of SIRT3 display features similar to the Warburg effect apparent in many cancer cells.

Previous studies have found that SIRT3 loss increases glucose uptake (Kim et al., 2010), yet, to our knowledge, the specific mechanism involved has not been elucidated. To test whether SIRT3 upregulates glycolysis as part of a compensatory response due to diminished oxidative capacity, we examined glucose uptake and lactic acid secretion in the presence of a mitochondrial respiratory inhibitor, rotenone, or an inhibitor of mitochondrial fatty acid oxidation, etomoxir. In WT cells, glycolysis is increased in the presence of both rotenone (Figures 1K and 1L) and etomoxir (Figures 1M and 1N).

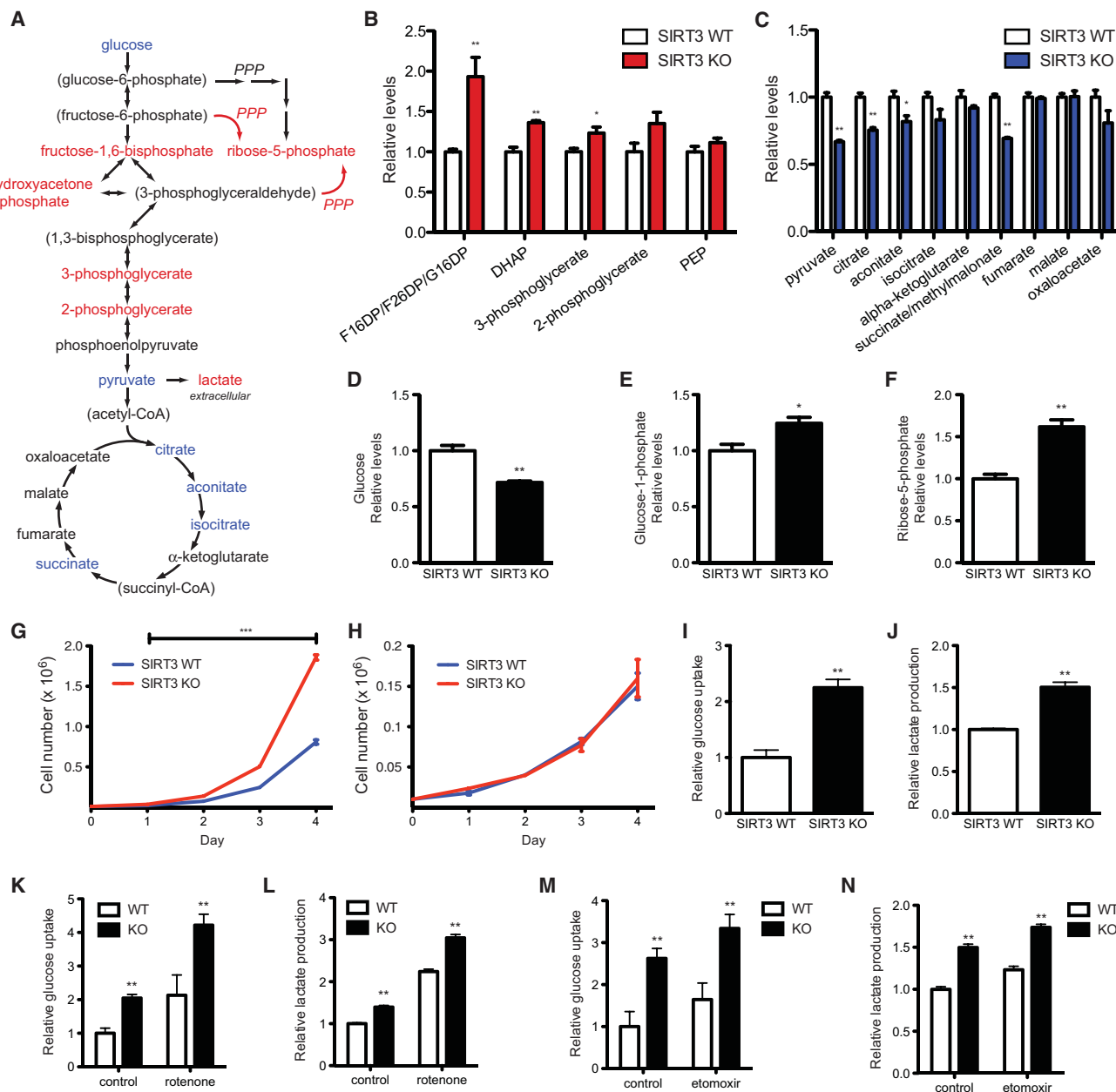


Figure 1. Metabolic Profiles of SIRT3 KO MEFs Reflect an Increase in Glycolytic Pathways and a Decrease in Mitochondrial Oxidative Metabolism

(A) Schematic illustrating the metabolites that are increased (red) or decreased (blue) in SIRT3 KO MEFs compared to SIRT3 WT MEFs ($n = 4$; $p < 0.1$). Metabolites in parentheses were not measured. The nonoxidative (red) and oxidative (black) arms of the PPP are shown. Levels of glycolytic intermediates (B), TCA cycle intermediates (C), glucose (D), glucose-1-phosphate (E), and ribose-5-phosphate (F). Growth curves of SIRT3 WT and KO MEFs ($n = 3$) cultured in media containing glucose (G) or galactose (H). Error bars, \pm SD (I–N) Glucose uptake and lactate production in SIRT3 WT and KO MEFs ($n = 6$). (I) Relative glucose uptake and (J) lactate production in SIRT3 WT and KO MEFs. (K) Relative glucose uptake and (L) relative lactate production in SIRT3 WT and KO MEFs incubated with or without 100 nM rotenone. (M) Glucose uptake and (N) lactate production in SIRT3 WT and KO MEFs cultured in the presence or absence of 50 μ g/ml etomoxir. Cells were treated with drugs for 24 hr before measuring glucose uptake and lactate. All error bars (except growth curves), \pm SEM. * $p < 0.05$; ** $p < 0.01$; *** $p < 0.001$. See also Figure S1.

Strikingly, glucose uptake and lactate production remain elevated in the SIRT3 KO cells even in the presence of oxidation inhibitors (Figures 1K–1N). These data demonstrate that up-regulated glycolysis in SIRT3 null cells does not result solely

from nonspecific compensation for decreased mitochondrial oxidative functions. Instead, these data indicate that, surprisingly, SIRT3 may regulate glycolysis via activation of a specific signaling pathway.

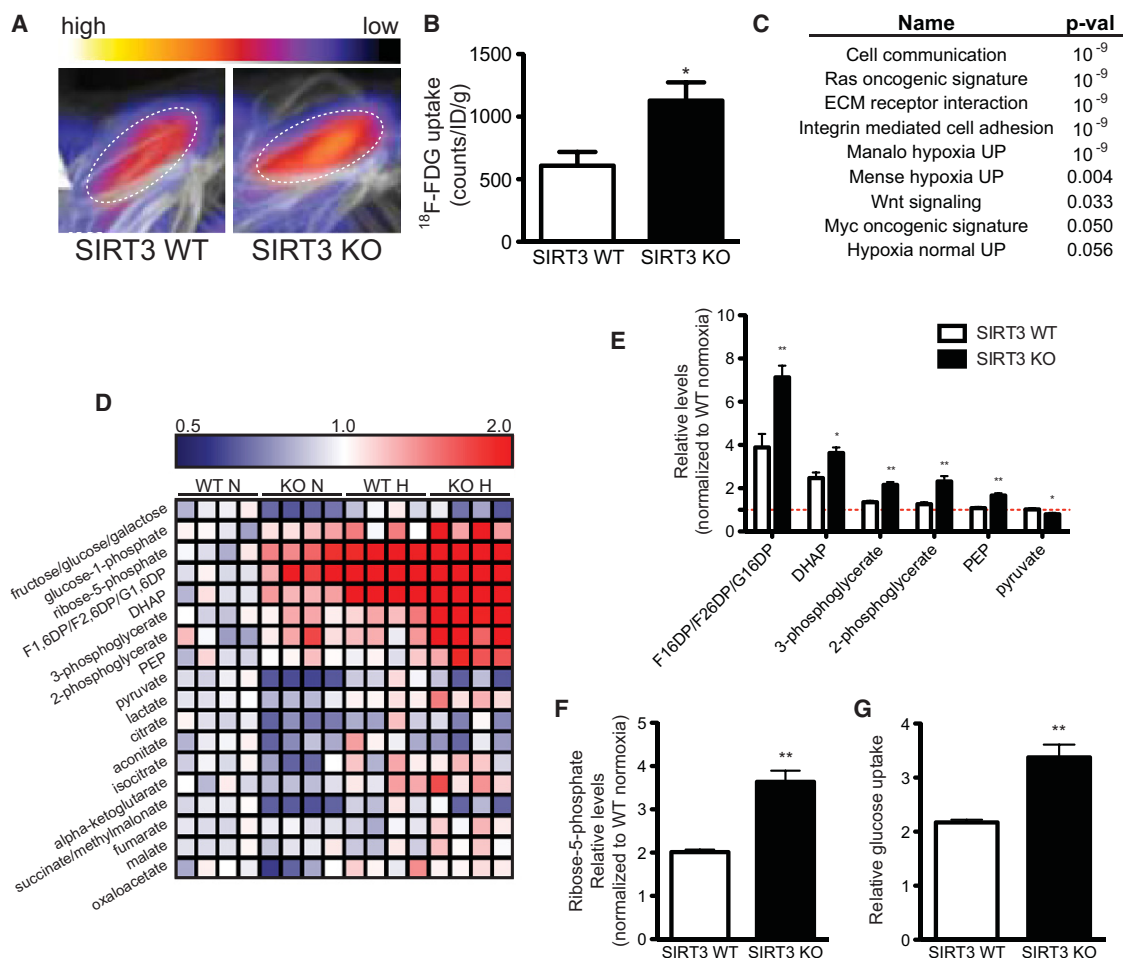


Figure 2. SIRT3 KO Mice Have Elevated Glucose Uptake and Hypoxic Signatures In Vivo

^{18}F -FDG uptake in the BAT of SIRT3 WT and KO mice was measured using PET/CT.

(A) Representative scans with color scale bar indicating relative levels of uptake from low (black) to high (white).

(B) Quantification of BAT ^{18}F -FDG uptake normalized to body weight ($n = 6$).

(C) GSEA of canonical pathways with the ranked genes list from most upregulated to most downregulated in SIRT3 KO BAT.

(D) Heat map comparing metabolite patterns of SIRT3 deletion and hypoxia. Red and blue indicate up- or downregulation, respectively. SIRT3 WT and KO MEFs ($n = 4$) were cultured in 21% O_2 (normoxia, N) or 1% O_2 for 12 hr (hypoxia, H), and metabolites were analyzed by LC-MS. Relative levels of glycolytic intermediates (E) and ribose-5-phosphate (F).

(G) Glucose uptake of MEFs cultured under hypoxia for 6 hr. Error bars, \pm SEM. * $p < 0.05$; ** $p < 0.01$.

See also Figure S2.

We next asked whether SIRT3 KO mice exhibited signs of increased glucose usage. We injected mice with ^{18}F -fluorodeoxyglucose (^{18}F -FDG) and scanned animals using positron emission tomography-computed tomography (PET/CT) in order to monitor glucose uptake. We looked specifically in brown adipose tissue (BAT), which exhibits high glucose uptake (Cannon and Nedergaard, 2004). In line with our cellular studies, we found that SIRT3 KO mice had an increase in ^{18}F -FDG uptake in BAT compared with WT mice (Figures 2A and 2B), even though the mass of BAT in SIRT3 KO mice was not larger than in WT mice (Figure S2A). Glucose uptake in BAT is regulated by the β -adrenergic pathway and is thus dramatically increased by cold exposure (Shimizu et al., 1991). We measured ^{18}F -FDG uptake in BAT of SIRT3 WT and KO mice after a 6-hr cold challenge and found that SIRT3 KO mice have higher ^{18}F -FDG

uptake both at room temperature and at 4°C (Figure 2B; Figure S2B), illustrating that SIRT3 WT and KO mice have a similar increase in BAT glucose uptake in response to β -adrenergic signaling. These differences in BAT glucose uptake occur independently of obvious changes in whole-body glucose homeostasis: we did not detect changes in blood glucose levels (Figure S2C) as reported previously (Lombard et al., 2007).

To examine mechanisms underlying increased glucose uptake in SIRT3 KO BAT, we performed genome-wide expression profiling on RNA isolated from BAT and performed gene set enrichment analysis (GSEA) using the ranked gene list from most upregulated to most downregulated in SIRT3 KO mice in order to identify the biological pathways most significantly altered by SIRT3 loss. Because SIRT3 is a mitochondrial deacetylase, we expected to see compensatory upregulation of

pathways involving mitochondrial function or energy production. To our surprise, SIRT3 loss upregulated pathways important in tumorigenesis. Strikingly, of the nine gene sets most significantly overrepresented in SIRT3 KO BAT, three were independently defined as gene sets induced by exposure to hypoxia (Figure 2C; Figure S2B). Hypoxia itself increases ^{18}F -FDG uptake (Clavo et al., 1995) and is associated with many transcriptional changes that result in increased glucose uptake and utilization (Brahimi-Horn et al., 2007). Thus, we hypothesized that the increase in glucose uptake in SIRT3 KO BAT could be explained by upregulation of the hypoxia response.

The similarity between gene signatures of SIRT3 KO mice and hypoxic cells was particularly notable because hypoxia induces a metabolic shift similar to that caused by loss of SIRT3, including a decrease in mitochondrial substrate oxidation and an increase in glycolysis (Semenza, 2010). To test the role of SIRT3 in hypoxia-induced metabolic reprogramming, we analyzed metabolites isolated from MEFs cultured at 21% O₂ (normoxia) or 1% O₂ (hypoxia) for 12 hr. Strikingly, we observed that the increase in glycolytic intermediates caused by hypoxia was similar to the effects of SIRT3 deletion (Figure 2D). Furthermore, hypoxia and SIRT3 loss had additive effects: whereas intermediates of glycolysis, glycogenolysis, and the PPP were elevated by hypoxia, levels of these metabolites were even higher in SIRT3 KO MEFs under these conditions (Figures 2E and 2F; Figure S2E). Consistent with the metabolite profiles, hypoxia increased glucose uptake in both cell lines, and SIRT3 KO or knockdown cells consumed even more glucose than control cells (Figure 2G; Figure S2F). Taken together, these data illustrate that SIRT3 loss and hypoxia result in similar metabolic shifts and implicate dysregulated activation of the hypoxia pathway as a cause of the metabolic reprogramming of SIRT3 null cells.

SIRT3 Opposes the Warburg Effect by Destabilizing HIF1 α

HIF1, the heterodimer of HIF1 α and HIF1 β , is the primary driver of increased glycolysis and lactate production during hypoxia (Gordan and Simon, 2007; Hu et al., 2003; Seagroves et al., 2001). Under conditions of low oxygen, HIF1 α is stabilized and promotes transcription of many genes crucial for the cellular response to hypoxia (Kaelin and Ratcliffe, 2008). Consequently, cells lacking HIF1 α fail to upregulate glycolytic enzymes and lactic acid production in response to hypoxia (Seagroves et al., 2001). Given the in vivo hypoxic gene signature of SIRT3 null BAT, in addition to the striking similarity between the mitochondrial-independent glycolytic profiles of SIRT3 KO MEFs and hypoxic cells, we reasoned that the mechanism by which SIRT3 regulates glycolysis involves HIF1 α . To test this idea we first investigated whether SIRT3 directly modulates HIF1 α stability under normoxic conditions. In the presence of high oxygen, HIF1 α is rapidly degraded and difficult to measure from cell lysates, but HIF1 α is detectable from isolated nuclei. Indeed, nuclei isolated from SIRT3-deficient cells during normoxia demonstrated elevated levels of HIF1 α relative to WT cells (Figure 3A). Likewise, when MEFs were cultured under 1% O₂, HIF1 α was stabilized earlier and to a higher degree in SIRT3 KO cells compared to WT cells in whole-cell lysates (Figure 3B). We obtained comparable results in HEK293T cells in which

SIRT3 expression was stably reduced by lentiviral expression of shRNA against SIRT3 (Figure 3C). Importantly, SIRT3 also regulates expression of HIF1 α target genes. Both the glucose transporter *Glut1* and hexokinase II (*Hk2*)—HIF1 α target genes that are critical for increased glucose uptake and catabolism via aerobic glycolysis or the PPP and are strongly implicated in tumorigenesis (O'Donnell et al., 2006; Tennant et al., 2010)—were elevated during hypoxia in SIRT3 KO MEFs and SIRT3 knockdown cells relative to control cells (Figure 3D; Figure S3A). Furthermore, the HIF1 α targets pyruvate dehydrogenase kinase 1 (*Pdk1*), lactate dehydrogenase A (*Ldha*), phosphoglycerate kinase (*Pgk1*), and vascular endothelial growth factor A (*Vegfa*) were significantly elevated in SIRT3 KO cells compared to WT cells during hypoxia (Figure 3D). Similar to the pattern we saw with metabolic intermediates of glycolysis, many of these genes were moderately elevated by SIRT3 loss under basal conditions (Figure S3B), and SIRT3 deletion and hypoxia had additive effects on expression of HIF1 α target genes (Figure 3D).

To test whether SIRT3 directly represses HIF1 α , we examined the levels of HIF1 α and its target genes in cells overexpressing SIRT3. SIRT3 overexpression clearly and reproducibly reduced the extent of HIF1 α stabilization in hypoxic cells (Figure 3E). Importantly, the induction of *GLUT1* and *HK2* during hypoxia was blunted by SIRT3 overexpression, demonstrating that SIRT3 directly inhibits HIF1 α function (Figure 3F). SIRT3 catalytic activity was required for the full repression of HIF1 α target genes: expression of a SIRT3 catalytic mutant did not significantly reduce hypoxic *GLUT1* expression (Figure S3C). Furthermore, using primary MEFs, we found that two SIRT3 KO lines exhibited increased *Glut1* expression relative to two WT lines, suggesting that SIRT3 can regulate HIF1 α activity in primary cell lines (Figure S3D). Taken together, the data show that SIRT3 controls the stabilization of HIF1 α and the induction of crucial HIF1 α target genes that coordinate aerobic glucose consumption.

Next, to examine the requirement for HIF1 α in the glycolytic shift observed in SIRT3 null cells, we used two separate shRNA constructs against HIF1 α to generate SIRT3 WT and KO MEFs with HIF1 α levels stably reduced (Figure S3E). We measured normoxic and hypoxic *Glut1* expression in these cell lines and found, as predicted, that control (shNS) SIRT3 KO MEFs demonstrated an exaggerated response to hypoxia, measured as the fold change in *Glut1* expression, compared to control WT MEFs (Figure 3G). In contrast, WT and SIRT3 KO MEFs expressing either shRNA against HIF1 α had comparable responses to hypoxia (Figure 3G; Figure S3F). Importantly, the increase in lactate production caused by SIRT3 deletion required HIF1 α both in normoxia and hypoxia (Figure 3H; and Figure S3G). Together, these data demonstrate that SIRT3 regulates aerobic glycolysis through HIF1 α .

To probe for evidence of increased HIF1 α activation in vivo, we measured levels of HIF1 α and HIF1 α target genes from tissues of SIRT3 WT and KO mice. Levels of HIF1 α protein and many HIF1 α target genes involved in glycolysis were significantly elevated in the BAT of SIRT3 KO mice (Figure 3I; Figure S3H–S3J), consistent with our studies demonstrating increased glucose uptake in SIRT3 KO BAT. Similarly, several HIF1 α target genes showed a trend of increased expression in SIRT3 KO heart (Figure 3I; Figure S3K).

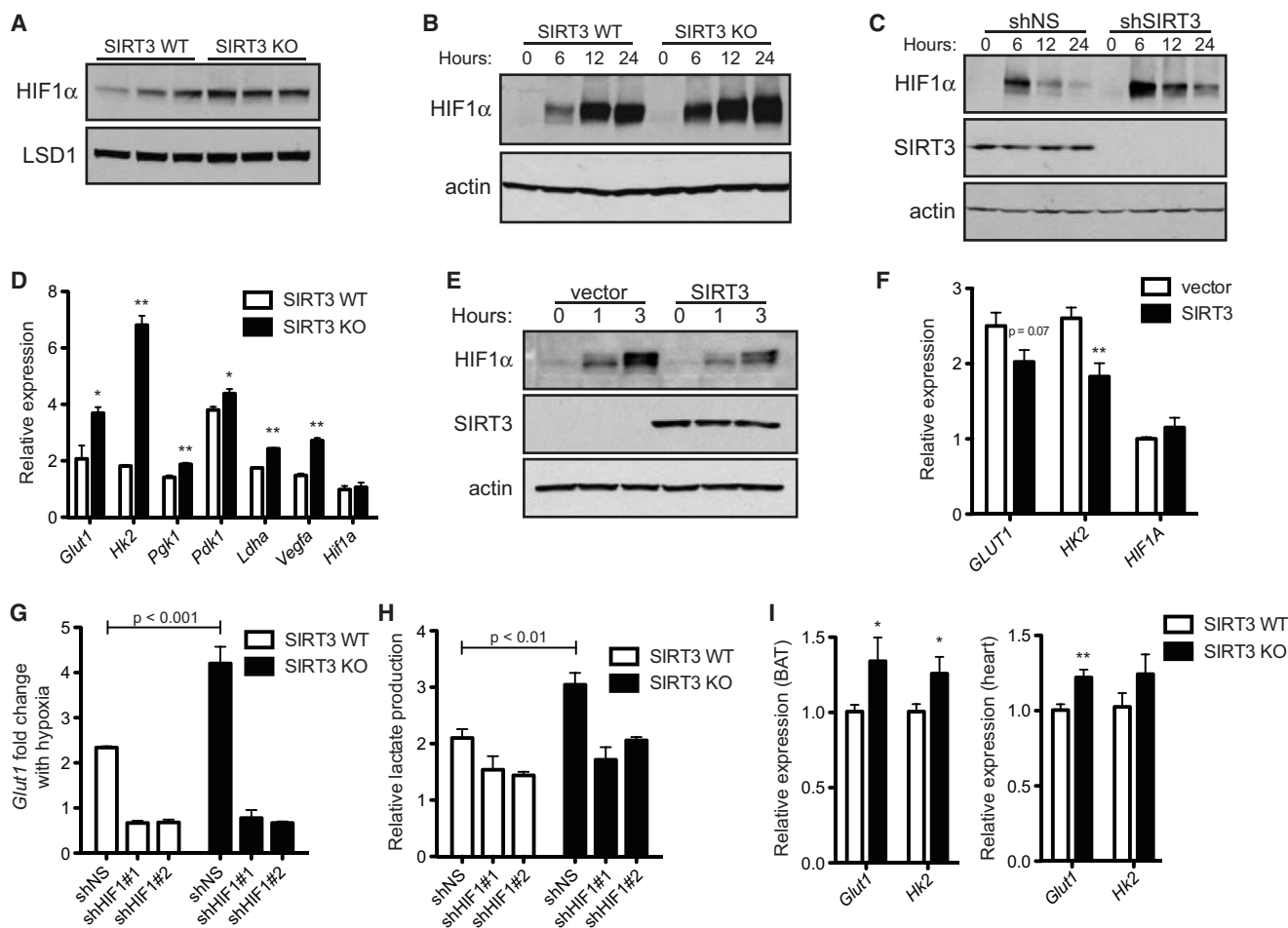


Figure 3. SIRT3 Regulates HIF1 α Stability

(A) Immunoblots of nuclear extracts from SIRT3 WT and KO MEFs cultured at 21% O₂.

(B and C) Immunoblots of MEFs (B) or HEK293T cells expressing control shRNA (shNS) or shRNA targeted against SIRT3 (C) cultured at 1% O₂ for the indicated times.

(D) HIF1 α target genes in SIRT3 WT and KO MEFs after 6 hr of hypoxia were measured by qRT-PCR and shown as a ratio of SIRT3 WT normoxia levels.

(E) Immunoblots of HEK293T cells stably overexpressing empty vector or SIRT3 cultured at 1% O₂ for the indicated times.

(F) Expression of HIF1 α target genes in HEK293T control and SIRT3-overexpressing cells after 6 hr of hypoxia.

(G) SIRT3 WT and KO MEFs expressing shNS or shRNA against HIF1 α (shHIF1#1,2) were cultured in normoxia or hypoxia (6 hr), and the fold change in *Glut1* levels was measured by qRT-PCR.

(H) Lactate produced by SIRT3 WT and KO MEFs expressing shNS or shHIF1 α after 6 hr of hypoxia expressed as a ratio of SIRT3 WT shNS normoxic controls. Significance was assessed by two-way ANOVA.

(I) Expression of *Glut1* and *Hk2* in the BAT (left) and heart (right) of SIRT3 WT and KO mice (n = 5–7) was measured by qRT-PCR. β -2-Microglobulin or Rps16 was used as an endogenous control for qRT-PCR. Error bars, \pm SEM (n = 4–6). *p < 0.05; **p < 0.01.

See also Figure S3.

The regulation of HIF1 α is complex and not completely understood (Kaelin and Ratcliffe, 2008). During normoxia, HIF1 α is hydroxylated at two proline residues by a family of oxygen-dependent prolyl hydroxylases (PHD1–3), enabling the tumor suppressor von Hippel-Lindau (vHL) to bind and target HIF1 α for ubiquitination and proteasomal degradation (Kaelin and Ratcliffe, 2008). Because we did not detect changes in HIF1 α mRNA levels (Figures 3D and 3F), we tested whether SIRT3 exerted a posttranslational effect on HIF1 α stability. SIRT1 binds HIF1 α and regulates its activity through direct deacetylation (Lim et al., 2010). To test whether SIRT3 might act through a similar mechanism, we immunoprecipitated SIRT1 or SIRT3 and probed

for interactions with HIF1 α . SIRT1, but not SIRT3, pulled down HIF1 α (Figure S4A), suggesting that SIRT3 does not interact with HIF1 α directly.

We next tested the hypothesis that SIRT3 regulates HIF1 α stability by modulating PHD activity by measuring the extent of HIF1 α hydroxylation. We assessed PHD activity in control and SIRT3 knockdown HEK293T cells by treating cells with the proteasomal inhibitor MG-132 (to prevent hydroxylated HIF1 α from being degraded) or with dimethylxylglycine (DMOG; to inhibit PHDs). Although SIRT3 knockdown cells accumulated more HIF1 α during MG-132 treatment, they had significantly less hydroxylated HIF1 α , indicating that PHD activity is lower in

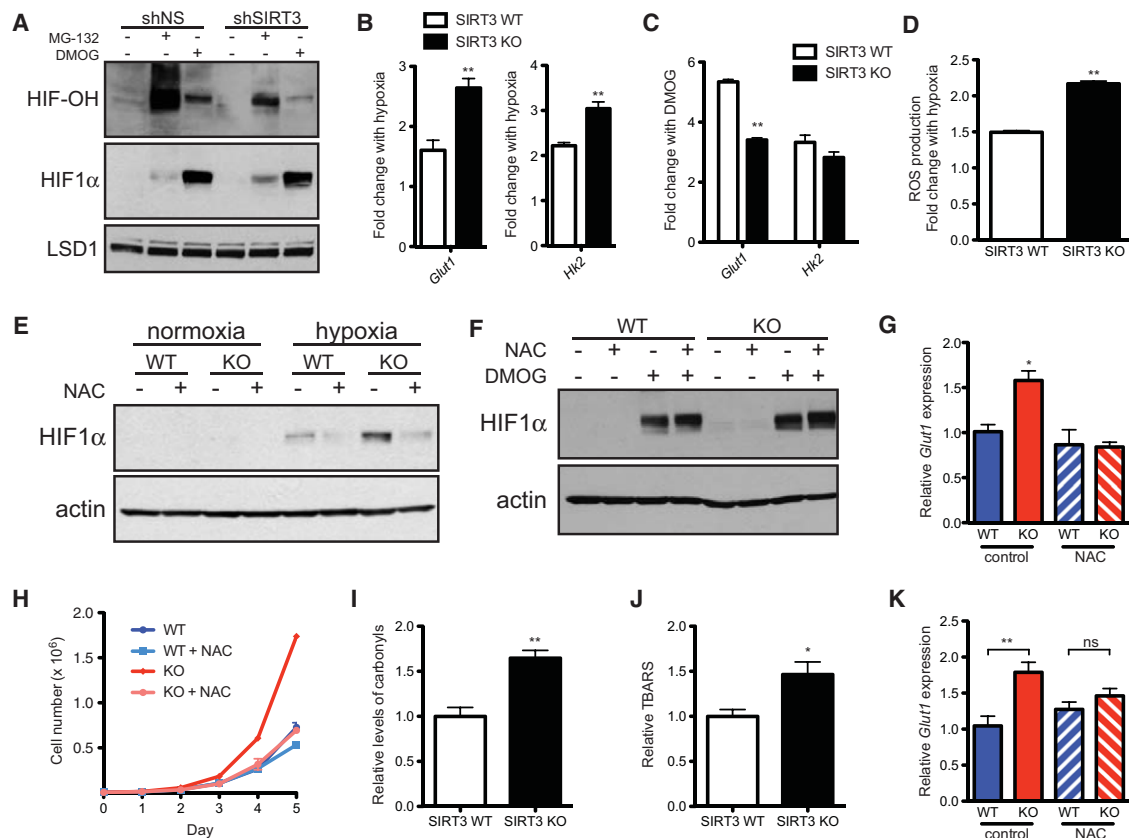


Figure 4. SIRT3 Regulates HIF1 α Stability through ROS

(A) Nuclear extracts from shNS and shSIRT3 HEK293T cells treated with or without 10 μ M MG-132 for 1 hr or 1 mM DMOG for 4 hr as indicated were immunoblotted with antibodies specific to hydroxylated HIF1 α (HIF-OH) or total HIF1 α .

(B) Fold induction of HIF1 α target genes in response to hypoxia (n = 6) measured by qRT-PCR. The ratio of hypoxic to normoxic gene expression is shown.

(C) Fold induction of *Glut1* and *Hk2* in response to DMOG treatment was measured by qRT-PCR, and the ratio of untreated to DMOG-treated gene expression is shown (n = 6).

(D) The increase in ROS production with hypoxia was calculated as the fold change in ROS in hypoxic cells relative to normoxic controls.

(E) Immunoblots of SIRT3 WT and KO MEFs incubated with 10 mM NAC and cultured under normoxia or hypoxia.

(F) Immunoblots of SIRT3 WT and KO MEFs cultured at 21% O₂ with 10 mM NAC or 1 mM DMOG as indicated.

(G) *Glut1* expression was measured by qRT-PCR in SIRT3 WT and KO MEFs (n = 5) that were incubated with 10 mM NAC and cultured under hypoxia. Significance was assessed by one-way ANOVA.

(H) Growth curves of SIRT3 WT and KO MEFs (n = 3) cultured in standard media or media supplemented with 10 mM NAC. Error bars, \pm SD.

(I and J) Protein carbonyls (I) and lipid peroxidation (J) were measured in BAT of SIRT3 WT and KO mice treated with 40 mM NAC. (n = 7).

(K) qRT-PCR analysis of *Glut1* expression in BAT of SIRT3 WT and KO mice treated with 40 mM NAC. β -2-Microglobulin or Rps16 was used as an endogenous control. Error bars (except for growth curves), \pm SEM. ns, nonsignificant. *p < 0.05; **p < 0.01.

See also Figure S4.

SIRT3 knockdown cells (Figure 4A). Similarly, SIRT3 WT MEFs demonstrated higher levels of HIF1 α hydroxylation than KO MEFs (Figure S4B). If SIRT3 influences HIF1 α stability through modulation of PHD activity, then treatment with the potent PHD inhibitor DMOG would overcome the effects of SIRT3 deletion and result in equivalent levels of HIF1 α stabilization in SIRT3 WT and KO cells. Indeed, we observed that at every time point examined, SIRT3 WT and KO MEFs have equal levels of HIF1 α stabilized in response to DMOG treatment (Figure S4C).

To confirm that SIRT3 influences HIF1 α through the PHDs, we performed a series of experiments comparing the effects of hypoxia and DMOG treatment on SIRT3 WT and KO MEFs. We observed that both hypoxia and DMOG stabilize HIF1 α and induce expression of HIF1 α target genes (Figures 4B and 4C).

The relative responses of SIRT3 WT and KO MEFs to hypoxia and DMOG underscore the PHDs as the point of regulation by SIRT3. During hypoxia, HIF1 α target genes are induced more strongly in SIRT3 KO cells, illustrating the physiological importance of SIRT3 in regulating the metabolic response to hypoxia (Figure 4B). In contrast, SIRT3 deletion represses the induction of HIF1 α target genes in response to DMOG (Figure 4C). These data support a model whereby PHD activity is already reduced in SIRT3 KO cells. Consequently, when PHD activity is potentially blocked by DMOG, SIRT3 KO cells have a smaller change in PHD activity and, thus, a smaller induction of HIF1 α target genes. Together, these results point to reduced PHD activity as the mechanism of increased HIF1 α expression in SIRT3-deficient cells.

Several intracellular signals, in addition to changes in oxygen concentration, are known to regulate PHD activity. Notably, ROS have been shown to inhibit the PHDs and stabilize HIF1 α (Gerald et al., 2004; Kaelin and Ratcliffe, 2008). Moreover, hypoxia triggers an increase in ROS production that is required for the hypoxic activation of HIF1 α (Chandel et al., 1998; Hama-naka and Chandel, 2009). Because SIRT3 is a well-known inhibitor of ROS (Kawamura et al., 2010; Kim et al., 2010; Kong et al., 2010; Sundaresan et al., 2009), we hypothesized that increased ROS in SIRT3-deficient cells would contribute to the inhibition of the PHDs. Thus, we tested whether SIRT3 loss would magnify the increase in ROS associated with hypoxia. We found that the hypoxia-triggered increase in ROS was significantly higher in SIRT3 KO MEFs (Figure 4D), providing a mechanistic explanation for why SIRT3 null cells have an exaggerated response to hypoxia.

Next, we treated cells with the antioxidant N-acetylcysteine (NAC) in order to probe the model that suppressing ROS could block the effects of SIRT3 deletion. Indeed, we observed that whereas SIRT3 KO MEFs had higher levels of HIF1 α during hypoxia, NAC treatment reduced HIF1 α to comparable levels in SIRT3 WT and KO MEFs (Figure 4E). In contrast, SIRT3 WT and KO MEFs have comparable levels of HIF1 α induced by DMOG (Figure 4F), and NAC could no longer destabilize HIF1 α in the presence of DMOG (Figure 4F; Figure S4D). As predicted by the decrease in HIF1 α observed in NAC-treated KO MEFs, NAC treatment restored *Glut1* expression in KO MEFs to WT levels (Figure 4G). Finally, to test whether increased ROS could underlie the proliferative phenotype of SIRT3 KO MEFs, we cultured cells with NAC and measured growth rates. Strikingly, we found that NAC rescued the increased proliferation of SIRT3 KO MEFs, restoring their growth to WT levels (Figure 4H). Thus, regulation of ROS by SIRT3 plays an important role in stabilization of HIF1 α and activation of glycolytic metabolism in SIRT3 null cells.

To examine the contribution of increased ROS to altered BAT metabolism in vivo, we first looked for evidence of increased ROS in SIRT3 KO tissues. We found that two measures of oxidative damage, protein carbonyls and lipid peroxidation, were significantly elevated in SIRT3 KO BAT (Figures 4I and 4J). Because antioxidant treatment rescued the HIF1 α -driven gene expression in cultured cells, we hypothesized that NAC treatment would reverse the glycolytic signature in SIRT3 KO tissues. To test this idea we treated mice with NAC for 1 month and measured expression of HIF1 α target genes in BAT. Strikingly, we found that NAC repressed expression of HIF1 α target genes in SIRT3 KO mice, but not in SIRT3 WT mice (Figure 4K; Figures S4E and S4F). These data demonstrate that increased ROS production in vivo contributes to enhanced glycolytic gene expression in SIRT3-deficient mice.

SIRT3 Loss Increases Glycolytic Signatures in Tumors

HIF1 α activity and aerobic glycolysis are strongly implicated in the Warburg effect (Semenza, 2010), and so we reasoned that SIRT3 may exert its tumor-suppressive activity by opposing the HIF1 α -mediated activation of the Warburg effect. Previously, SIRT3 deletion was shown to increase colony formation in a soft agar colony growth assay (Kim et al., 2010). To investigate the contribution of HIF1 α to this tumorigenic phenotype, we trans-

formed primary MEFs by expressing the Ras and E1a oncogenes and then stably knocked down HIF1 α . As previously shown (Kim et al., 2010), we found that SIRT3 loss increased colony formation (Figure 5A). Importantly, knock down of HIF1 α rescued the increased colony formation of SIRT3 KO cells (Figure 5A). Furthermore, SIRT3 WT and KO MEFs formed colonies at equivalent rates when cultured in media containing galactose instead of glucose (Figure S5A), suggesting that colony formation required glucose metabolism. Taken together, these data suggest that the metabolic reprogramming mediated by SIRT3 via HIF1 α could be an important contributor of the tumor-suppressive role of SIRT3.

Next, we performed xenograft assays with the transformed MEFs in order to probe the metabolic status of SIRT3 null tumors. As has previously been shown (Kim et al., 2010), we found that tumors lacking SIRT3 had a growth advantage: tumors formed from 64% of KO injections, but only 27% of WT injections and tumors lacking SIRT3 grew faster and were bigger than WT tumors (Figures S5B–S5F). Because tumors are subject to intermittent hypoxia (Gatenby and Gillies, 2004), we examined expression of rate-limiting glycolytic genes in the xenograft tumors. Strikingly, HIF1 α target genes were elevated in SIRT3 KO tumors (Figure 5B); SIRT3 KO tumors also showed higher levels of GLUT1 protein (Figure 5C). Taken together, these data suggest that increased levels of glycolytic enzymes, perhaps as part of a heightened response to hypoxia, provide a growth advantage for tumor cells lacking SIRT3 in vivo.

SIRT3 Is Deleted in Many Human Cancers

Our data indicate that SIRT3 may regulate tumor cell metabolism and anabolic growth pathways. In order to determine the relevance of SIRT3 in human cancers, we first examined the copy number variations of SIRT3 that are associated with the progression of multiple types of human cancer (Beroukhi et al., 2010). Strikingly, at least one copy of the *SIRT3* gene is deleted in 20% of all human cancers and 40% of breast and ovarian cancers present in the data set (Figure 5D). *SIRT3* is significantly focally deleted (deletions of less than a chromosome arm) across all cancers, and focal deletions of *SIRT3* were especially frequent in breast and ovarian tumors (Figure 5D). In contrast, *SIRT4* and *SIRT5* were not significantly focally deleted in any of the 14 subtypes analyzed (Figure 5E; data not shown). *TP53*, a tumor suppressor known to be frequently deleted in many human cancers, is included as a control (Fisher, 2001) (Figure 5E; Figures S4G and S4H). Our analysis of copy number changes at the *SIRT3* locus revealed no evidence of focal amplifications across 14 types of cancer. Most of the genomic *SIRT3* deletions are heterozygous, and *SIRT3* deletion frequencies are similar to the well-known breast cancer tumor suppressors, *BRCA1* and *BRCA2*, which are heterozygously deleted in 43% and 40% of human breast cancers, respectively (data not shown). Intriguingly, the peak region of deletion that includes *SIRT3* (11p15.5) does not contain any known tumor suppressor (Beroukhi et al., 2010).

Because breast cancers exhibited exceptionally high frequency of SIRT3 deletions compared to other tumor types (Figure 5D) (Kim et al., 2010), we further examined SIRT3 in human breast cancers. Elevated HIF1 α expression in breast carcinomas is associated with tumor aggressiveness and poor

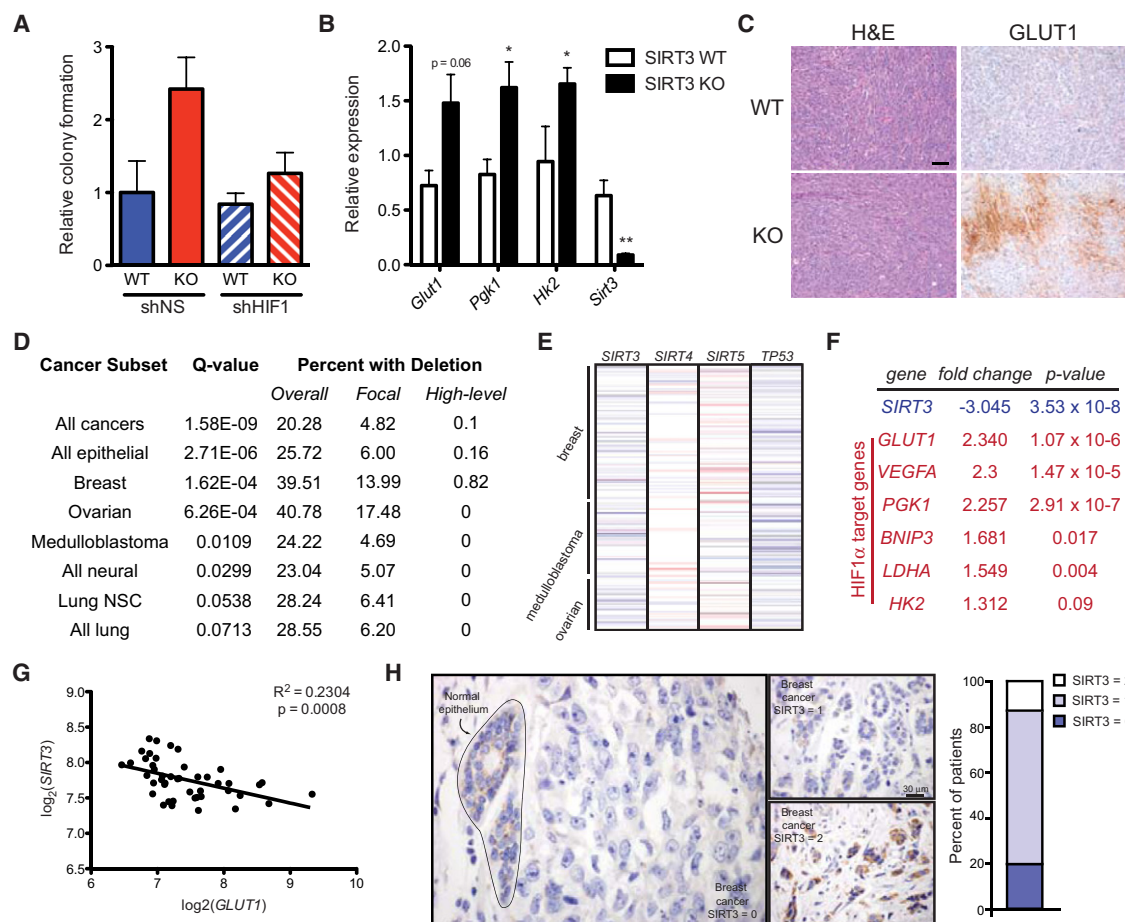


Figure 5. SIRT3 Is Significantly Deleted in Human Breast Cancer

(A) Soft agar assays using transformed SIRT3 WT and KO MEFs expressing shNS or shRNA against HIF1 α (shHIF1) (n = 4).

(B) Quantitative RT-PCR on RNA isolated from xenograft tumors and normalized to expression of 36B4.

(C) H&E (left) and immunohistochemical analysis of GLUT1 expression (right) in xenograft tumors. One representative pair of contralateral tumors is shown. Scale bar, 50 μ m.

(D) Table summarizing SIRT3 deletion frequency across a panel of human tumors.

(E) Schematic of copy number changes at the SIRT3-5 and TP53 loci. Amplifications are shown in red; deletions are shown in blue.

(F) Expression levels of SIRT3 and several HIF1 α target genes were determined using the Oncomine cancer microarray database (<http://www.oncomine.org>) in normal versus breast cancers.

(G) Linear regression of SIRT3 and GLUT1 across the panel of normal and breast cancer samples described in (F).

(H) Representative image of SIRT3 expression in normal breast epithelium and in breast tumor cells as assessed by immunohistochemistry. SIRT3 levels were classified as absent (0), weak scattered (1), or positive as strong (2) compared to normal epithelium, and the percentage of patients classified in each category is depicted in histogram at right. Error bars, \pm SEM (n = 4–6). *p < 0.05; **p < 0.01.

See also Figure S5.

prognosis (Chaudary and Hill, 2006). Many breast cancer cells exhibit increased glycolysis, and expression of GLUT1 is a characteristic feature of many breast cancer biopsies (Rivenzon-Segal et al., 2003). In xenograft models, SIRT3 loss increases expression of HIF1 α target genes and results in strong GLUT1 expression (Figures 5B and 5C). Thus, we looked for a relationship between SIRT3 loss and HIF1 α targets in human breast cancer. Gene expression profiling of seven normal breast samples and 40 ductal breast carcinomas revealed that SIRT3 expression is significantly reduced ($p = 3.53 \times 10^{-8}$) in breast carcinomas (Richardson et al., 2006) (Figure 5F). Moreover, several HIF1 α target genes—most notably GLUT1—were significantly increased in the same data set (Figure 5F). We further analyzed

the correlation between SIRT3 and GLUT1 expression in individual samples from this data set and found that SIRT3 is significantly inversely correlated with GLUT1 ($p = 0.0008$) (Figure 5G). Our results demonstrate that SIRT3 loss is associated with increased expression of HIF1 α target genes in vivo and in human breast cancer and provide a metabolic link between SIRT3 deletion and breast cancer tumorigenesis.

To confirm that SIRT3 expression is reduced in human breast cancers, we analyzed SIRT3 protein levels by immunohistochemistry in normal breast epithelium in addition to a large panel of human breast cancer tissue. Out of 46 patient samples, only six demonstrated SIRT3 staining that was positive or as strong as SIRT3 staining in normal epithelium (Figure 5H). Strikingly,

87% of patients showed decreased or undetectable SIRT3 staining in adjacent cancer tissue, and 20% of patients showed no detectable SIRT3 (Figure 5H). Similarly, gene expression profiling of an independent set of human breast cancer samples (Richardson et al., 2006) revealed that 25% of breast cancers exhibited at least a 6-fold reduction in the mRNA of *SIRT3* compared to normal breast epithelium (Figure S5I). This independent data set provides additional validation for the observation that *SIRT3* is deleted in human tumors (Figure 5D) (Beroukhi et al., 2010). Furthermore, an earlier high-resolution analysis of copy number variation in 171 human breast tumors similarly found significant reduction in *SIRT3* copy number (Chin et al., 2007). These findings also support those of Kim et al. (2010), who first reported that SIRT3 KO mice develop mammary tumors and that SIRT3 levels were decreased in human breast cancer.

The studies of SIRT3 expression in human cancers suggest that SIRT3 may function as a tumor suppressor in part by preventing the metabolic shift that facilitates tumor growth. In order to examine whether SIRT3 can actively repress the Warburg effect in tumor cells, we stably overexpressed SIRT3 in three independent breast cancer cell lines: MCF7, T47D, and CAMA1 (Figure S6A). We analyzed the glucose uptake and lactate secretion in cells during hypoxia in order to simulate the tumor microenvironment. We found that SIRT3 repressed both lactate production and glucose uptake in every cell line tested (Figures 6A and 6B). These data clearly demonstrate that overexpression of SIRT3 in tumor cells is sufficient to reverse the metabolic shift associated with the Warburg effect.

Because SIRT3 robustly suppressed glucose uptake and lactate production in the CAMA1 cells, we chose to further analyze these cell lines. To examine the contribution of complex I activity or fatty acid oxidation on these phenotypes, we measured glucose uptake and lactate production in the presence of rotenone and etomoxir. Both rotenone and etomoxir increased glucose uptake and lactate production to a similar degree in both control and SIRT3-overexpressing cell lines, indicating that the repression of glycolysis by SIRT3 is independent of the influence of SIRT3 on fatty acid oxidation or complex I activity (Figures 6C–6F).

We next examined whether SIRT3 repressed HIF1 α in CAMA1 cells. SIRT3 overexpression strongly reduced HIF1 α protein levels and expression of HIF1 α target genes in hypoxic cells (Figures 6G and 6H). Moreover, when we examined the fold change of HIF1 α targets in response to hypoxia or DMOG treatment, we found the inverse of the results using SIRT3 KO MEFs. SIRT3 overexpression blunted the response to hypoxia (Figure 6I) while increasing the response to DMOG (Figure 6J). This is consistent with a model of elevated PHD activity in SIRT3-overexpressing cells and illustrates the importance of SIRT3 in regulating the physiological response to hypoxia at the level of the PHDs.

Next, we tested the hypothesis that SIRT3-mediated control of glucose metabolism could influence cancer cell proliferation. SIRT3 overexpression significantly repressed proliferation of CAMA1 cells cultured in high glucose (Figure 6K). Remarkably, control and SIRT3-expressing cells proliferated at similar rates when cultured in media containing galactose instead of glucose (Figure 6L). These data illustrate that SIRT3 regulates cancer

cell growth by influencing the use of glucose for anabolic processes.

DISCUSSION

In this study we demonstrate that SIRT3 regulates cellular metabolism through HIF1 α with important implications for tumor cell growth. Previously, it has been shown that SIRT3 is a mitochondrial deacetylase that activates multiple metabolic enzymes and promotes mitochondrial substrate oxidation and ATP production (Finkel et al., 2009; Verdin et al., 2010). Our study shows that SIRT3 additionally controls glycolytic metabolism (Figures 1 and 2) by regulating the stability and activity of HIF1 α (Figure 3). We find that elevated ROS in SIRT3 null cells contributes to increased HIF1 α stabilization and activity (Figure 4). Significantly, loss of *SIRT3* in human tumor samples correlates with glycolytic gene expression, highlighting the potential importance of SIRT3-mediated metabolic reprogramming in human cancers (Figure 5). This idea is further validated by the finding that SIRT3 represses the Warburg effect in human breast cancer cell lines (Figure 6). Taken together, these data provide a mechanism whereby SIRT3 functions as a tumor suppressor by regulating glycolytic and anabolic metabolism (Figure 6M).

Our findings are consistent with previous work showing that SIRT3 functions as a tumor suppressor through regulation of ROS (Kim et al., 2010). Kim et al. (2010) found that elevated ROS in the absence of SIRT3 increased genomic instability, promoting a tumor-permissive environment. We propose that SIRT3 loss and increased ROS also promote tumorigenesis by altering global cellular metabolism. In this study we demonstrate that elevated ROS stabilizes HIF1 α , increasing glucose uptake and catabolism and, thus, providing the metabolic precursors necessary to fuel a high rate of proliferation. Importantly, we demonstrate that increased glycolysis is not simply compensation for reduced mitochondrial oxidative capacity. Rather, SIRT3 actively regulates cellular glucose metabolism by activating a specific signaling node (Figures 1K–1N and 6C–6F). Thus, taken together, our study and the one by Kim et al. (2010) show that SIRT3 loss results in a double-edged sword for tumor cells—creating an environment of increased genome instability as well as HIF1 α activation, enabling increased glycolysis and cellular growth.

Recent studies have shed light on the mechanism through which SIRT3 regulates cellular ROS. Several groups have provided evidence that SIRT3 can influence transcription of antioxidant genes through activation of FoxO3a (Kim et al., 2010; Sundaresan et al., 2009), although we did not find a difference in *Sod2* expression under our culture conditions (Figure S6B). Additionally, SIRT3 can directly target IDH2, influencing cellular redox status, and SOD2, activating mitochondrial ROS scavenging (Qiu et al., 2010; Someya et al., 2010; Tao et al., 2010). As a result, SIRT3 can directly influence mitochondrial metabolism and ROS generation through deacetylation of multiple substrates. At the same time the ROS by-product of reduced SIRT3 activity acts as a retrograde signal to reprogram cellular metabolism.

Our studies reveal the profound impact of SIRT3 function on glycolysis and tumor cell metabolism. SIRT3 appears to be

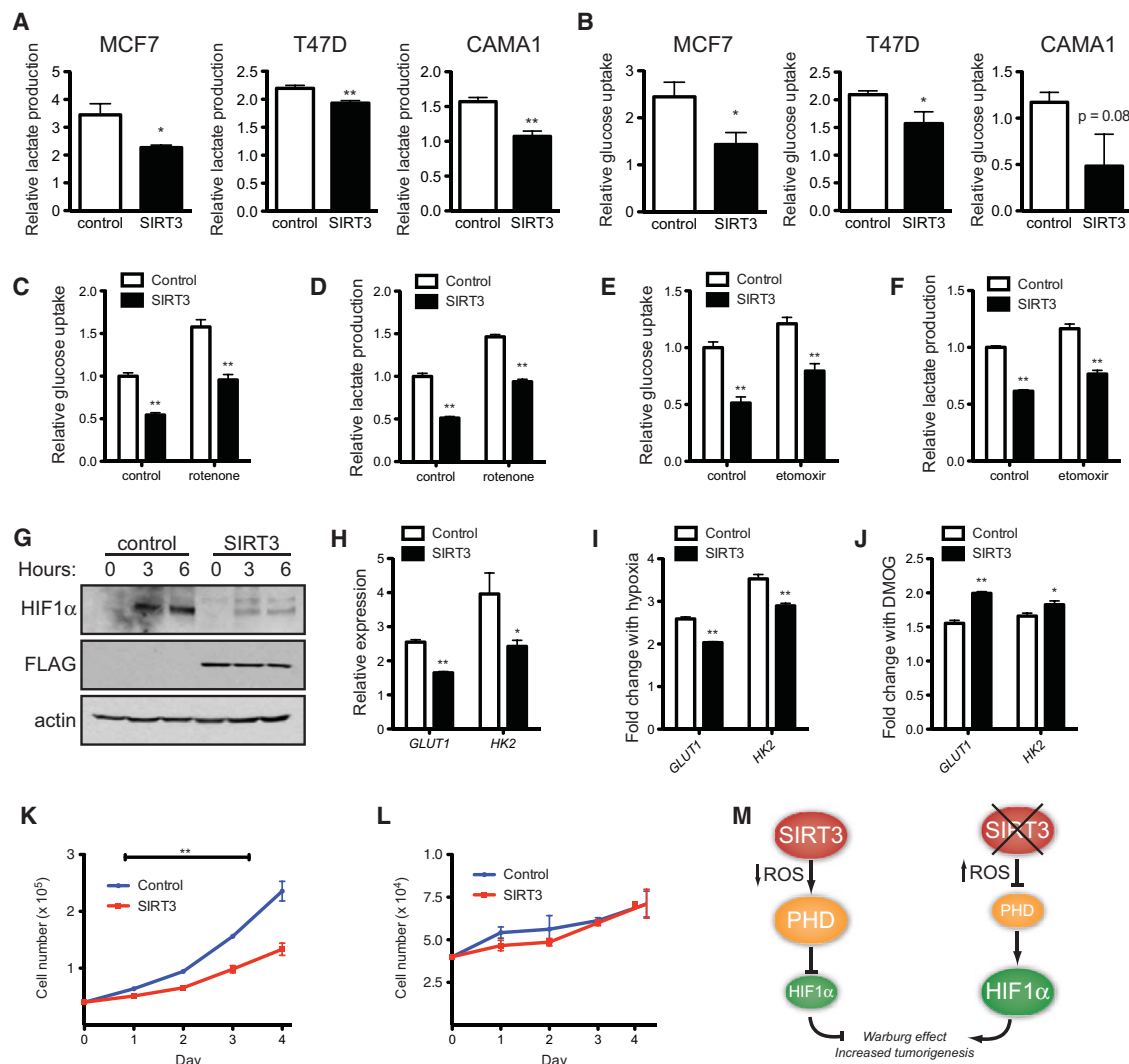


Figure 6. SIRT3 Suppresses the Warburg Effect in Human Breast Cancer Cells

(A) Lactate production and (B) glucose consumption of MCF7, T47D, and CAMA1 cells stably expressing empty vector or SIRT3 and cultured under hypoxia expressed as a ratio of empty vector-normoxic controls.

(C) Relative glucose uptake and (D) relative lactate production in CAMA1 control or SIRT3-overexpressing cells incubated with or without 100 nM rotenone.

(E) Glucose uptake and (F) lactate production in CAMA1 cell lines cultured in the presence or absence of 50 μ g/ml etomoxir.

(G) Immunoblots of CAMA1 cells stably expressing control vector or SIRT3-FLAG cultured at 1% oxygen for the indicated times.

(H) qRT-PCR of HIF1 α target genes in CAMA1 cells cultured at 1% oxygen.

(I) Induction of HIF1 α target genes in response to hypoxia measured by qRT-PCR in CAMA1 cells. The ratio of normoxic to hypoxic gene expression in each cell line is shown.

(J) Induction of HIF1 α target genes in response to 1 mM DMOG treatment measured by qRT-PCR in CAMA1 cells. The ratio of untreated to DMOG-treated gene expression in each cell line is shown.

(K and L) Growth curves of CAMA1 cells (n = 3) cultured in glucose (K) or galactose (L). Error bars, \pm SD. (M) Schematic of the regulation of HIF1 α and the Warburg effect by SIRT3. β -2-Microglobulin was used as an endogenous control for qRT-PCR. Error bars (except for growth curves), \pm SEM. *p < 0.05; **p < 0.01.

See also Figure S6.

decreased in human breast cancers (Figure 5) (Beroukhi et al., 2010; Chin et al., 2007; Kim et al., 2010; Richardson et al., 2006). It will be important for future work to examine the impact of SIRT3 on each stage of tumorigenesis in mechanistic detail. Given the function of SIRT3 in breast cancer (Kim et al., 2010), in addition to our findings that SIRT3 can reprogram cellular metabolism (Figures 1 and 2), we propose that the glycolytic switch evident in cells lacking SIRT3 will contribute to tumorigen-

esis, particularly in breast cancers. In support of this idea, we show that SIRT3 can directly repress the Warburg effect in three independent breast cancer cell lines (Figure 6). In sum, our studies illustrate that SIRT3 functions as a tumor suppressor, in part by regulating cellular metabolism through HIF1 α . These findings suggest that the regulation of tumor cell metabolism by SIRT3 could provide an important area for cancer diagnosis or therapeutic intervention.

EXPERIMENTAL PROCEDURES

Metabolite Profiling

Metabolites were extracted in ice-cold methanol, and endogenous metabolite profiles were obtained using two liquid chromatography-tandem mass spectrometry (LC-MS) methods as described (Luo et al., 2007). Data were acquired using a 4000 QTRAP mass spectrometer (Applied Biosystems/Sciex). Multi-Quant software (Applied Biosystems/Sciex) was used for analysis. Metabolite levels were normalized to protein content, which was determined by performing a Bradford assay (Bio-Rad) on a duplicate set of cells treated identically to the experimental cells.

Lactate and Glucose Measurements

Glucose and lactate levels in culture media were measured using the BioProfile FLEX analyzer (Nova Biomedical) and normalized to cell number or using the Lactate Reagent Kit (Trinity Biosciences). Fresh media were added to a 6-well plate of subconfluent cells, and lactate concentration in the media was measured 30–60 min (Lactate Reagent Kit) or 6–24 hr (BioProfile Analyzer) later and normalized to the number of cells in each well.

ROS Measurement

Cellular ROS was measured according to published protocols (Eruslanov and Kusmartsev, 2010). Briefly, cells were washed with PBS and incubated with 5 μ M CM-H₂DCFDA (Invitrogen) for 30 min. Cells were trypsinized, and mean FL1 fluorescence was measured by flow cytometry.

Oxidative Damage

Protein carbonyl content was determined as previously described (Levine et al., 1994). Levels of lipid peroxidation were determined using a modified version of the thiobarbituric acid reactive substances (TBARS) procedure (Ernst et al., 1968).

Animal Studies

Animal studies were performed according to protocols approved by the Institutional Animal Care and Use Committee, the Standing Committee on Animals at Harvard. Male 129Sv SIRT3 WT and KO (Lombard et al., 2007) littermates (a generous gift from Dr. Fred Alt) fed a normal chow diet (PicoLab Diet 5053) were used for all studies. PET/CT studies were performed at the Longwood SAIF (Boston). Eight to 10-month-old male mice were injected with 300 μ Ci ¹⁸F-FDG and imaged 1 hr later on PET/CT. For cold challenge, mice were injected after 6 hr at 4°C. Results were analyzed using InVivoScope software. For NAC studies, drinking water was supplemented with 40 mM NAC for 4 weeks prior to sacrifice. For xenograft studies, 5 \times 10⁶ or 7.5 \times 10⁶ SIRT3 WT or KO MEFs transformed by expression of the Ras and E1a oncogenes were mixed with Matrigel (BD Biosciences) and injected subcutaneously into nude mice (6- to 9-week-old males; Taconic Farms). Each mouse was injected with WT cells on one flank and KO cells on the other flank. Tumor size was measured every 2 days, and tumors were dissected and weighed after 4 weeks.

Immunohistochemistry

Tumors were fixed in 4% paraformaldehyde and embedded in paraffin. Sections were stained with hematoxylin and eosin (H&E) in accordance with standard procedures. Immunohistochemistry was performed using antibodies against GLUT1 (Alpha Diagnostic) according to manufacturer instructions. A tissue microarray (TMA) was constructed as previously published using a fully automated Beecher Instrument, ATA-27. The study cohort comprised of breast carcinoma, consecutively ascertained at the Memorial Sloan-Kettering Cancer Center (MSKCC) between 1993 and 2005. Use of tissue samples was approved with an Institutional Review Board Waiver, and samples were de-identified prior to analysis. All breast cancer biopsies were evaluated at MSKCC, and the histological diagnosis was based on H&E. One to several cores contained normal breast duct epithelium. The TMA was stained with an antibody against SIRT3 (Cell Signaling) with pretreatment conditions including citrate buffer and microwave at 1:100 dilution. Cores were scored by a pathologist (J.T.-F.), and tumor staining intensity was compared to normal breast duct epithelium as: 0, tumor showing no staining; 1, tumor weaker than normal epithelium; and 2, tumor of equal or stronger intensity compared to normal ductal epithelium (Figure S5J). Histologic immunohistochemical

images for Figure 5H were obtained with the Olympus AH2 Microscope Camera from Center Valley, PA. Image acquisition and processing software were performed using an Olympus DP12 camera and software, and Adobe Photoshop 7.0. Magnification was \times 400 (scale bar \sim 30 μ m).

Statistics

Unpaired two-tailed Student's *t* tests were performed unless otherwise noted. All experiments were performed at least two to three times.

ACCESSION NUMBERS

The SIRT3 BAT microarray has been deposited in a GEO database with accession number GSE27309.

SUPPLEMENTAL INFORMATION

Supplemental Information includes Supplemental Experimental Procedures and six figures and can be found with this article online at doi:10.1016/j.ccr.2011.02.014.

ACKNOWLEDGMENTS

We thank Fred Alt for the SIRT3 KO mice. We thank Elaine Lunsford and the Longwood SAIF for the PET/CT imaging and analysis, Kristin Waraska and the Harvard Biopolymers Facility for running the TaqMan assays, Kelly Dakin and Bruce Yankner for use of their hypoxic incubator, Natalie German and Maren Shapiro for technical assistance, Ditte Lee for help with mouse work, and Maria Jiao in the Laboratory of Comparative Pathology, Sloan Kettering Institute, for immunohistochemical technical assistance. We thank Kevin Haggis, Carla Kim, and Karen Cichowski for critical reading of the manuscript, and David Gius, Sandra Ryeom, Gaelle Laurent, Lenny Guarente, and Eric Bell for helpful discussion. L.W.S.F. is supported by a National Science Foundation graduate research fellowship. A.C. is supported by the Ramón y Cajal award. M.C.H. is supported in part by NIH grant AG032375, and funding from the Paul F. Glenn Foundation, the Alexander and Margaret Stewart Trust, and the Muscular Dystrophy Association.

Received: October 22, 2010

Revised: January 13, 2011

Accepted: February 17, 2011

Published: March 14, 2011

REFERENCES

- Ahn, B.H., Kim, H.S., Song, S., Lee, I.H., Liu, J., Vassilopoulos, A., Deng, C.X., and Finkel, T. (2008). A role for the mitochondrial deacetylase Sirt3 in regulating energy homeostasis. *Proc. Natl. Acad. Sci. USA* 105, 14447–14452.
- Beroukhim, R., Mermel, C.H., Porter, D., Wei, G., Raychaudhuri, S., Donovan, J., Barretina, J., Boehm, J.S., Dobson, J., Urashima, M., et al. (2010). The landscape of somatic copy-number alteration across human cancers. *Nature* 463, 899–905.
- Brahimi-Horn, M.C., Chiche, J., and Pouyssegur, J. (2007). Hypoxia signalling controls metabolic demand. *Curr. Opin. Cell Biol.* 19, 223–229.
- Cannon, B., and Nedergaard, J. (2004). Brown adipose tissue: function and physiological significance. *Physiol. Rev.* 84, 277–359.
- Chandel, N.S., Maltepe, E., Goldwasser, E., Mathieu, C.E., Simon, M.C., and Schumacker, P.T. (1998). Mitochondrial reactive oxygen species trigger hypoxia-induced transcription. *Proc. Natl. Acad. Sci. USA* 95, 11715–11720.
- Chaudary, N., and Hill, R.P. (2006). Hypoxia and metastasis in breast cancer. *Breast Dis.* 26, 55–64.
- Chin, S.F., Teschendorff, A.E., Marioni, J.C., Wang, Y., Barbosa-Morais, N.L., Thorne, N.P., Costa, J.L., Pinder, S.E., van de Wiel, M.A., Green, A.R., et al. (2007). High-resolution aCGH and expression profiling identifies a novel genomic subtype of ER negative breast cancer. *Genome Biol.* 8, R215.
- Christofk, H.R., Vander Heiden, M.G., Harris, M.H., Ramanathan, A., Gerszten, R.E., Wei, R., Fleming, M.D., Schreiber, S.L., and Cantley, L.C. (2008). The M2

- splice isoform of pyruvate kinase is important for cancer metabolism and tumour growth. *Nature* 452, 230–233.
- Cimen, H., Han, M.J., Yang, Y., Tong, Q., Koc, H., and Koc, E.C. (2010). Regulation of succinate dehydrogenase activity by SIRT3 in mammalian mitochondria. *Biochemistry* 49, 304–311.
- Clavo, A.C., Brown, R.S., and Wahl, R.L. (1995). Fluorodeoxyglucose uptake in human cancer cell lines is increased by hypoxia. *J. Nucl. Med.* 36, 1625–1632.
- Denkert, C., Budczies, J., Weichert, W., Wohlgemuth, G., Scholz, M., Kind, T., Niesporek, S., Noske, A., Buckendahl, A., Dietel, M., and Fiehn, O. (2008). Metabolite profiling of human colon carcinoma—deregulation of TCA cycle and amino acid turnover. *Mol. Cancer* 7, 72.
- Duvel, K., Yecies, J.L., Menon, S., Raman, P., Lipovsky, A.I., Souza, A.L., Triantafellow, E., Ma, Q., Gorski, R., Cleaver, S., et al. (2010). Activation of a metabolic gene regulatory network downstream of mTOR complex 1. *Mol. Cell* 39, 171–183.
- Ernster, L., Nordenbrand, K., Orrenius, S., and Das, M.L. (1968). Microsomal lipid peroxidation. *Hoppe Seyler's Z. Physiol. Chem.* 349, 1604–1605.
- Eruslanov, E., and Kusmartsev, S. (2010). Identification of ROS using oxidized DCFDA and flow-cytometry. *Methods Mol. Biol.* 594, 57–72.
- Finkel, T., Deng, C.X., and Mostoslavsky, R. (2009). Recent progress in the biology and physiology of sirtuins. *Nature* 460, 587–591.
- Fisher, D.E. (2001). The p53 tumor suppressor: critical regulator of life & death in cancer. *Apoptosis* 6, 7–15.
- Gatenby, R.A., and Gillies, R.J. (2004). Why do cancers have high aerobic glycolysis? *Nat. Rev. Cancer* 4, 891–899.
- Gerald, D., Berra, E., Frapart, Y.M., Chan, D.A., Giaccia, A.J., Mansuy, D., Pouyssegur, J., Yaniv, M., and Mechta-Grigoriou, F. (2004). JunD reduces tumor angiogenesis by protecting cells from oxidative stress. *Cell* 118, 781–794.
- Gordan, J.D., and Simon, M.C. (2007). Hypoxia-inducible factors: central regulators of the tumor phenotype. *Curr. Opin. Genet. Dev.* 17, 71–77.
- Gottlieb, E., and Tomlinson, I.P. (2005). Mitochondrial tumour suppressors: a genetic and biochemical update. *Nat. Rev. Cancer* 5, 857–866.
- Hamanaka, R.B., and Chandel, N.S. (2009). Mitochondrial reactive oxygen species regulate hypoxic signaling. *Curr. Opin. Cell Biol.* 21, 894–899.
- Hirayama, A., Kami, K., Sugimoto, M., Sugawara, M., Toki, N., Onozuka, H., Kinoshita, T., Saito, N., Ochiai, A., Tomita, M., et al. (2009). Quantitative metabolome profiling of colon and stomach cancer microenvironment by capillary electrophoresis time-of-flight mass spectrometry. *Cancer Res.* 69, 4918–4925.
- Hirschey, M.D., Shimazu, T., Goetzman, E., Jing, E., Schwer, B., Lombard, D.B., Grueter, C.A., Harris, C., Biddinger, S., Ilkayeva, O.R., et al. (2010). SIRT3 regulates mitochondrial fatty-acid oxidation by reversible enzyme deacetylation. *Nature* 464, 121–125.
- Hu, C.J., Wang, L.Y., Chodosh, L.A., Keith, B., and Simon, M.C. (2003). Differential roles of hypoxia-inducible factor 1 α (HIF-1 α) and HIF-2 α in hypoxic gene regulation. *Mol. Cell Biol.* 23, 9361–9374.
- Kaelin, W.G., Jr., and Ratcliffe, P.J. (2008). Oxygen sensing by metazoans: the central role of the HIF hydroxylase pathway. *Mol. Cell* 30, 393–402.
- Kawamura, Y., Uchijima, Y., Horike, N., Tonami, K., Nishiyama, K., Amano, T., Asano, T., Kurihara, Y., and Kurihara, H. (2010). Sirt3 protects in vitro-fertilized mouse preimplantation embryos against oxidative stress-induced p53-mediated developmental arrest. *J. Clin. Invest.* 120, 2817–2828.
- Kim, H.S., Patel, K., Muldoon-Jacobs, K., Bisht, K.S., Aykin-Burns, N., Pennington, J.D., van der Meer, R., Nguyen, P., Savage, J., Owens, K.M., et al. (2010). SIRT3 is a mitochondria-localized tumor suppressor required for maintenance of mitochondrial integrity and metabolism during stress. *Cancer Cell* 17, 41–52.
- Kong, X., Wang, R., Xue, Y., Liu, X., Zhang, H., Chen, Y., Fang, F., and Chang, Y. (2010). Sirtuin 3, a new target of PGC-1 α , plays an important role in the suppression of ROS and mitochondrial biogenesis. *PLoS ONE* 5, e11707.
- Levine, R.L., Williams, J.A., Stadtman, E.R., and Shacter, E. (1994). Carbonyl assays for determination of oxidatively modified proteins. *Methods Enzymol.* 233, 346–357.
- Lim, J.H., Lee, Y.M., Chun, Y.S., Chen, J., Kim, J.E., and Park, J.W. (2010). Sirtuin 1 modulates cellular responses to hypoxia by deacetylating hypoxia-inducible factor 1 α . *Mol. Cell* 38, 864–878.
- Lombard, D.B., Alt, F.W., Cheng, H.L., Bunkenborg, J., Streeper, R.S., Mostoslavsky, R., Kim, J., Yancopoulos, G., Valenzuela, D., Murphy, A., et al. (2007). Mammalian Sir2 homolog SIRT3 regulates global mitochondrial lysine acetylation. *Mol. Cell Biol.* 27, 8807–8814.
- Lu, X., Bennet, B., Mu, E., Rabinowitz, J., and Kang, Y. (2010). Metabolomic changes accompanying transformation and acquisition of metastatic potential in a syngeneic mouse mammary tumor model. *J. Biol. Chem.* 285, 9317–9321.
- Luo, B., Groenke, K., Takors, R., Wandrey, C., and Oldiges, M. (2007). Simultaneous determination of multiple intracellular metabolites in glycolysis, pentose phosphate pathway and tricarboxylic acid cycle by liquid chromatography-mass spectrometry. *J. Chromatogr. A* 1147, 153–164.
- Marroquin, L.D., Hynes, J., Dykens, J.A., Jamieson, J.D., and Will, Y. (2007). Circumventing the Crabtree effect: replacing media glucose with galactose increases susceptibility of HepG2 cells to mitochondrial toxicants. *Toxicol. Sci.* 97, 539–547.
- O'Donnell, J.L., Joyce, M.R., Shannon, A.M., Harmey, J., Geraghty, J., and Bouchier-Hayes, D. (2006). Oncological implications of hypoxia inducible factor-1 α (HIF-1 α) expression. *Cancer Treat. Rev.* 32, 407–416.
- Qiu, X., Brown, K., Hirschey, M.D., Verdin, E., and Chen, D. (2010). Calorie restriction reduces oxidative stress by SIRT3-mediated SOD2 activation. *Cell Metab.* 12, 662–667.
- Richardson, A.L., Wang, Z.C., De Nicolo, A., Lu, X., Brown, M., Miron, A., Liao, X., Iglehart, J.D., Livingston, D.M., and Ganesan, S. (2006). X chromosomal abnormalities in basal-like human breast cancer. *Cancer Cell* 9, 121–132.
- Rivenzon-Segal, D., Boldin-Adamsky, S., Seger, D., Seger, R., and Degani, H. (2003). Glycolysis and glucose transporter 1 as markers of response to hormonal therapy in breast cancer. *Int. J. Cancer* 107, 177–182.
- Schlicker, C., Gertz, M., Papatheodorou, P., Kachholz, B., Becker, C.F., and Steegborn, C. (2008). Substrates and regulation mechanisms for the human mitochondrial sirtuins Sirt3 and Sirt5. *J. Mol. Biol.* 382, 790–801.
- Seagroves, T.N., Ryan, H.E., Lu, H., Wouters, B.G., Knapp, M., Thibault, P., Laderoute, K., and Johnson, R.S. (2001). Transcription factor HIF-1 is a necessary mediator of the pasteure effect in mammalian cells. *Mol. Cell Biol.* 21, 3436–3444.
- Semenza, G.L. (2010). HIF-1: upstream and downstream of cancer metabolism. *Curr. Opin. Genet. Dev.* 20, 51–56.
- Shimizu, Y., Nikami, H., and Saito, M. (1991). Sympathetic activation of glucose utilization in brown adipose tissue in rats. *J. Biochem.* 110, 688–692.
- Someya, S., Yu, W., Hallows, W.C., Xu, J., Vann, J.M., Leeuwenburgh, C., Tanokura, M., Denu, J.M., and Prolla, T.A. (2010). Sirt3 mediates reduction of oxidative damage and prevention of age-related hearing loss under caloric restriction. *Cell* 143, 802–812.
- Sundaresan, N.R., Gupta, M., Kim, G., Rajamohan, S.B., Isbatan, A., and Gupta, M.P. (2009). Sirt3 blocks the cardiac hypertrophic response by augmenting Foxo3a-dependent antioxidant defense mechanisms in mice. *J. Clin. Invest.* 119, 2758–2771.
- Tao, R., Coleman, M.C., Pennington, J.D., Ozden, O., Park, S.H., Jiang, H., Kim, H.S., Flynn, C.R., Hill, S., Hayes McDonald, W., et al. (2010). Sirt3-mediated deacetylation of evolutionarily conserved lysine 122 regulates MnSOD activity in response to stress. *Mol. Cell* 40, 893–904.
- Tennant, D.A., Duran, R.V., and Gottlieb, E. (2010). Targeting metabolic transformation for cancer therapy. *Nat. Rev. Cancer* 10, 267–277.
- Tong, X., Zhao, F., and Thompson, C.B. (2009). The molecular determinants of de novo nucleotide biosynthesis in cancer cells. *Curr. Opin. Genet. Dev.* 19, 32–37.
- Vander Heiden, M.G., Cantley, L.C., and Thompson, C.B. (2009). Understanding the Warburg effect: the metabolic requirements of cell proliferation. *Science* 324, 1029–1033.
- Verdin, E., Hirschey, M.D., Finley, L.W., and Haigis, M.C. (2010). Sirtuin regulation of mitochondria: energy production, apoptosis, and signaling. *Trends Biochem. Sci.* 35, 669–675.
- Warburg, O. (1956). On the origin of cancer cells. *Science* 123, 309–314.
- Zhao, S., Lin, Y., Xu, W., Jiang, W., Zha, Z., Wang, P., Yu, W., Li, Z., Gong, L., Peng, Y., et al. (2009). Glioma-derived mutations in IDH1 dominantly inhibit IDH1 catalytic activity and induce HIF-1 α . *Science* 324, 261–265.